Application to biology and technology of the scanning tunneling microscope operated in air at ambient pressure

by A. M. Baró
R. Miranda
J. L. Carrascosa

We have investigated the operation of the scanning tunneling microscope (STM) in air at atmospheric pressure, thus permitting the imaging of samples without the need for subjecting them to a vacuum environment. Clearly, this may be of practical importance for many types of samples having biological and technological interest. Imaging of biological samples has been found to be possible after deposition onto a flat structureless conducting substrate (highly oriented pyrolytic graphite). Three-dimensional profiles of structures derived from the virus designated as bacteriophage ϕ29 could thus be obtained. Other profiles have been obtained which indicate applicability to surfaces of technological interest: for example, in the measurement of the surface roughness of industrial components with increased precision, suggesting use of the STM as a new standard instrument for that purpose.

Introduction

The STM has evolved from the use in 1981 of a sophisticated magnetically levitating unit [1] to maintain the distance between a sample and probe tip within the subnanometer range required to achieve vacuum tunneling. Since then, less complex mechanical isolation arrangements have been found to be adequate for that purpose [2]. Initially, use was made of high vacua to keep the electrode surfaces free of contamination. Subsequently, to examine clean surfaces, ultrahigh vacua were used, although it was clear that such vacua were not needed to utilize vacuum tunneling [3].

The feasibility of electron tunneling in air at ambient pressure was first demonstrated through use of a "squeezable" tunneling junction [4]. Attention in our laboratory has been devoted to exploring the potential of STM operation under such an air ambient condition. Initial emphasis was on stability and resolution aspects. The STM

used for that purpose was similar to the one developed by Binnig and Rohrer [5]. In air at ambient pressure, a thin oxide layer should develop on the metallic tip and on most samples. In addition, contaminant layers will most likely deposit on each. In contrast to other electron-microscopic techniques, in which use is made of electron beams, the electrons which are active in the STM are localized to the tip and the sample. Hence, gas phase molecules traversing the gap should not influence the tunneling process. We have observed a stability decrease if gap voltages greater than 2 to 3 volts are used—probably because of desorption of molecules by the applied field.

Figure 1 shows an example of an STM image which can be obtained in air at ambient pressure. The image is of an exfoliated surface of pyrolytic graphite. A step having an estimated height of 7 Å can be seen—in good agreement with the bulk lattice parameter of graphite ($2c = 6.7$ Å). Other larger steps can also be seen. Similar images on pyrolytic graphite have been reported previously [6]. The lateral and vertical resolutions are estimated, respectively, to be of the order of 8 and 1 Å.

The possibility of operating the STM in air opens new possibilities regarding the types of samples which it can be used to investigate. The resolution which is obtained is somewhat poorer than that obtained under vacuum conditions, but is still suitable for detecting features of atomic dimensions. In this paper, we describe results we have obtained using representative samples of biological and technological interest.

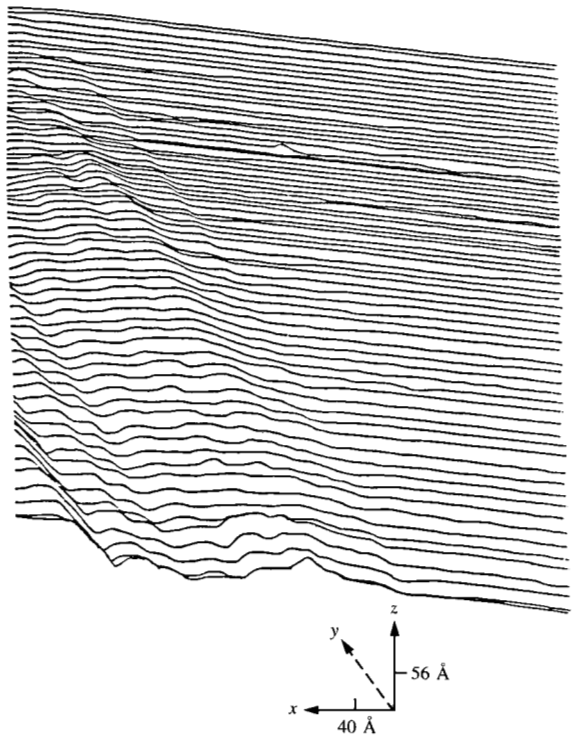

Figure 1

STM image of a highly oriented pyrolytic graphite surface. The graphite sample was exfoliated and the image obtained at atmospheric pressure. The left part of the image clearly shows steps on the surface. Most of the surface was atomically flat over a span of thousands of Å.

Biological samples

During the past fifty years transmission electron microscopy (TEM) has been used extensively to perform structural studies of biological samples at the molecular level. That technique is, however, not free from limitations which result from its inherent nature and associated sample preparation requirements. For example: 1) examination of three-dimensional objects requires reconstruction from images of two-dimensional sections (not more than 0.1 μm thick) or two-dimensional projections (if the object is small enough); 2) because of the small atomic weights of elements constituting biological material, biological samples are relatively transparent to the electron beam, necessitating the use of high electron doses which can damage such samples; and 3) containment is required within a chamber in which a vacuum is maintained in order to retain the collimation of the electron beam. In the case of biological samples, these requirements lead to the need for chemical agents to prevent vacuum drying, the need to add contrast by staining, and the preferable use of a crystalline array of target objects to lower the electron dose. Although very useful, the resolution which is obtained is limited to about 20 Å and fidelity is lost because the samples which are examined differ appreciably from the original biological objects. These considerations motivated our investigation of the applicability of the STM to the study of biological samples.

The requirement for a flat conducting structureless substrate was fulfilled by using a freshly cleaved pyrolytic graphite substrate of the type used to obtain Figure 1. Such a substrate contains flat regions which are free of significant surface defects for spans of thousands of Å. The samples of biological material were dialyzed against 0.2 M ammonium bicarbonate (containing 0.1% glycerol). This procedure removes salts of low-molar-mass contaminants, thus rendering the samples clear and in a uniform liquid environment. Furthermore, ammonium bicarbonate is volatile and, after drying, does not leave salt residues. Adhesion of the dialyzed samples to the graphite surface was achieved by drop deposition. A control experiment showed that no additional structure was introduced by this procedure.

We have deposited [6] two types of biological samples which were prepared from the virus designated as

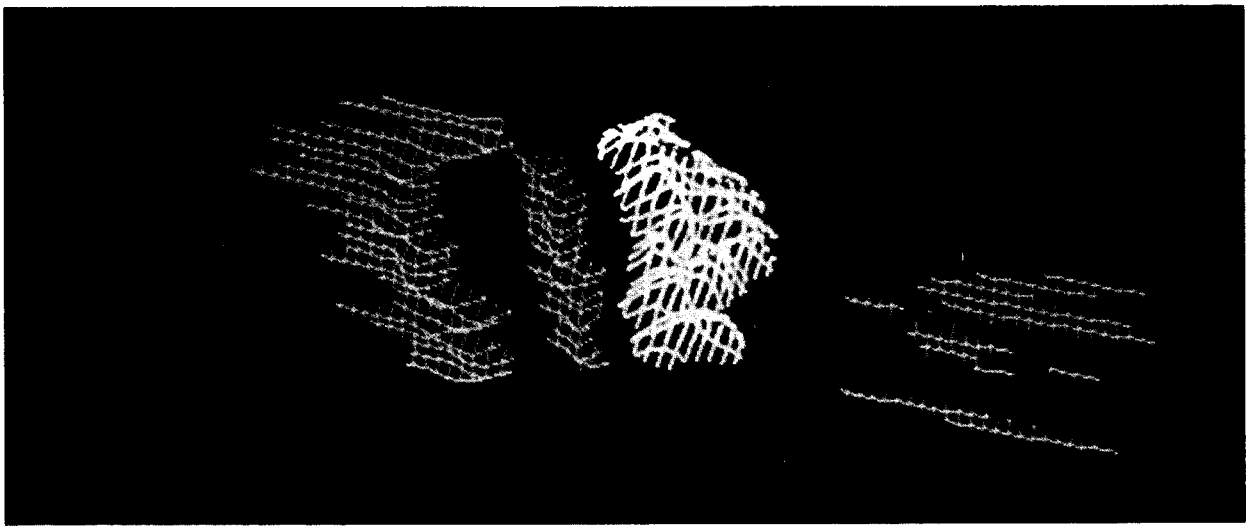

Figure 2

STM image, after image processing, of the upper collar of a bacteriophage $\phi 29$ particle. The image was obtained after deposition onto pyrolytic graphite and air-drying. It consists mainly of a ring about 160 Å in diameter and a central hole. The walls surrounding the hole are about 100 Å in height. The regions depicted in white, yellow, green, and blue contain, in that order, decreasing amounts of z-corrugation.

bacteriophage $\phi 29$. That bacteriophage is composed of a prolate icosahedral head (about 400 × 300 Å) and a complex tail (about 400 Å in length) [7, 8].

Figure 2 shows an STM image obtained (after image processing) of the upper collar of the $\phi 29$. The image processing was based on correlating each scan with its successive scan and compressing the y-axis to obtain cylindrical symmetry. Several characteristic features can be observed. The most important is a central hole which can be correlated with one which was observed using TEM [9]. To the left, there is a ring about 150 Å in diameter which can be correlated with the circular structure in the TEM work. The wall surrounding the central hole shows structure. The diameter of the ring is not uniform but changes from scan to scan. These changes can be tentatively correlated with the TEM observation of 12-fold symmetry. The right side of the image is different. Particularly striking is the disappearance of the ring structure. In order to understand this, we notice that the height of the left portion of the image is lower by about 30 Å than that of the right portion, indicating the presence of a step. It is reasonable to regard the step as a preferred site for the connector to reside. The same step would probably adsorb glycerol more actively, thus preventing the resolving of the structure to the right.

Images obtained from the second type of sample are shown in **Figure 3**. We have reported elsewhere [6] that we have been able to obtain scans which appear to traverse the head-tail axis of a DNA-containing $\phi 29$ particle. That figure contains examples of such scans. The total head-tail axis length is about 800 Å and the maximum corrugation in the z-direction is about 200 Å. Vacuum tunneling may have been possible because of some conductivity which exists inside the biological material. Parts (a) and (b) were taken successively over the same region, thus indicating good reproducibility and that the sample was not altered as a result of exposure to the STM.

Samples of technological interest

In this section, we present some examples of the applicability of the STM to the study of materials of technological interest.

Surface finishing of any machined part plays an important role in determining its subsequent mechanical properties. Because it can be used in air, the STM should be useful for the characterization of changes in surface topography resulting from a variety of surface treatments: hand-lapping, superfinishing, electropolishing, or ion implantation. At present, the accepted instrument for measuring surface roughness measurements of materials is a stylus instrument [10]. The latter has a 0.1-μm lateral resolution, thus limiting the minimum measurable wavelength of rugosity to that distance. The STM has recently been shown to be suitable for obtaining information on surface rugosity with unprecedented resolution [11].

A topographic image of a class "0" standard block gauge obtained with the STM is depicted in **Figure 4**. The block is used to calibrate industrial micrometers and has been hand-lapped. A fairly regular rugosity with an average roughness value of 200 Å, essentially aligned with the (known) direction of polishing, is observed. The average lateral

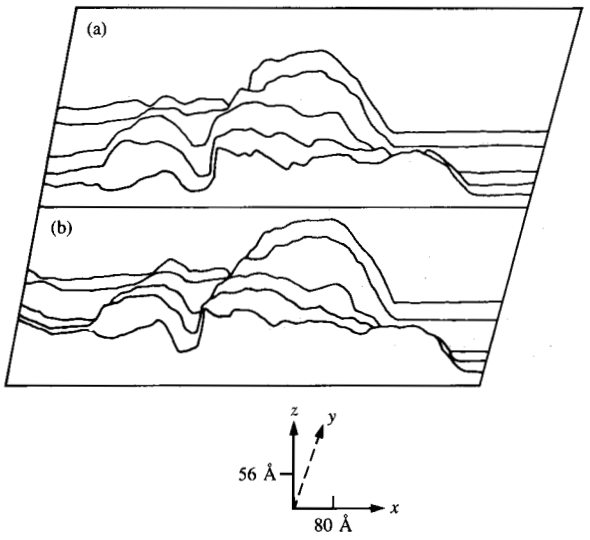

Figure 3

STM images of a DNA-containing bacteriophage $\phi 29$ particle. The scans appear to traverse the head-tail axis of the particle. The height of the DNA-containing head is about 200 Å, somewhat smaller than its lateral dimensions, as expected after the flattening induced by air-drying. The images in (a) and (b) were obtained in succession, indicating good reproducibility and that the sample was not altered by being subjected to STM examination.

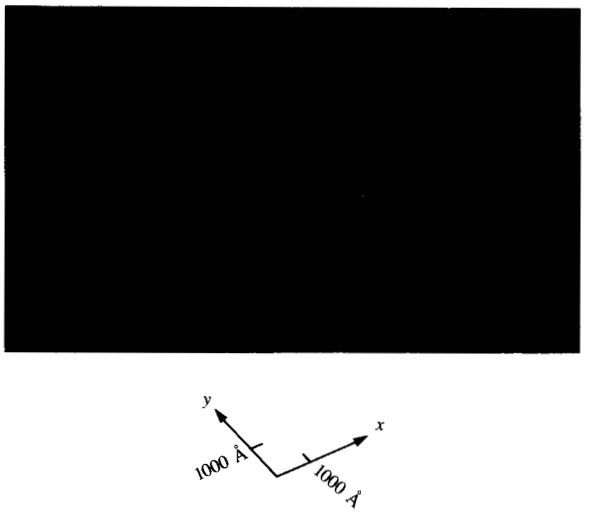

Figure 4

STM image of standard block gauge; taken at a tunneling voltage of 560 mV and a current of 6 nA. The wavy structure is in the polishing direction.

wavelength of the features observed is about 0.1 μm. This level of roughness, which has been referred to as granular roughness [10], is not measurable by other instruments. The capability to detect roughness at such a level may be important, for example, in connection with industrial tools because of a possible stress enhancement at associated granular structures. A trend in the field of surface finish metrology is towards increasing precision in roughness specification. We consider the air-operated version of the STM as an instrument which should be useful for that purpose.

The conductivity of a thin film is limited by electron scattering by phonons, lattice defects, grain boundaries, and at the surfaces of the film [12]. Of relevance here is that the upper surface of very thin films might be highly inhomogeneous because of island nucleation processes during the early stages of film growth. The use of the STM to obtain information on the surface topology of such a film is illustrated in **Figure 5**, which shows an STM image of a polycrystalline film of Pt deposited in high vacuum onto an exfoliated mica substrate [13]. The substrate was kept at room temperature during deposition and the thickness of the film was estimated to be 50–100 Å using a quartz crystal microbalance.

The structure of vacuum-deposited metal films is known to depend on many parameters [14]: the nature of the

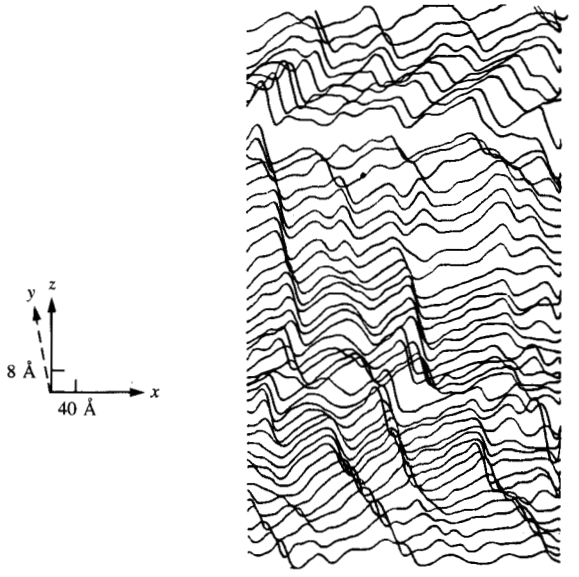

Figure 5

STM image of a Pt film, 50–100 Å in thickness, which was vacuum-deposited onto exfoliated mica; taken at a voltage of 0.5 V (tip negative) and a current of 6 nA.

substrate, evaporation rate, pressure and composition of the gas phase, film thickness, etc., but probably a major factor is the reduced temperature ($\tau = T/T_m$, i.e., the ratio of the

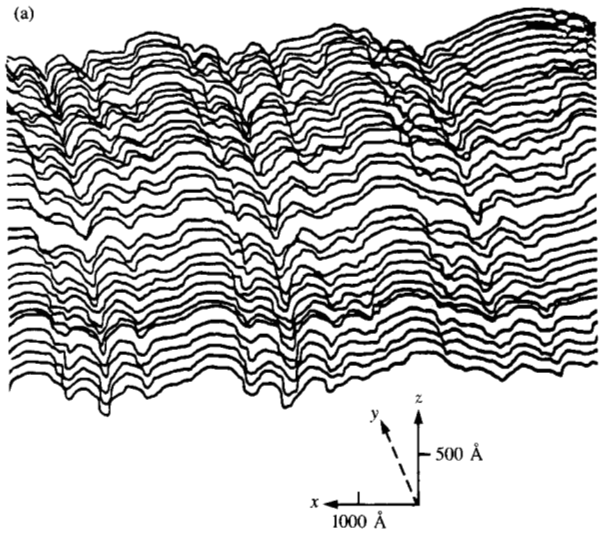

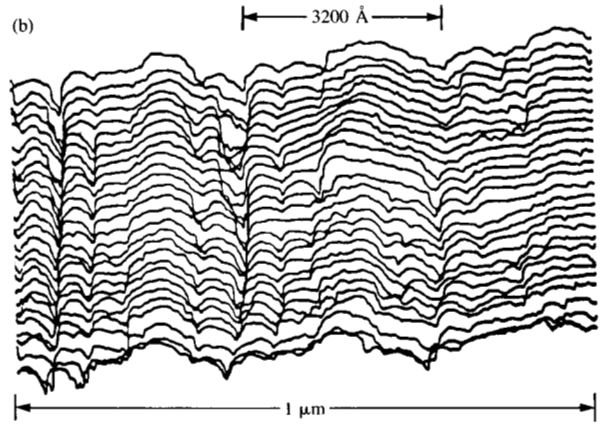

Figure 6

STM images of a p-type Si(100) sample which was preferentially etched to expose (111) surfaces in a triangular-appearing profile; taken at a voltage of 2.7 V (tip negative) and a current of 4 nA. Scanning was over an area of 1 μm × 0.2 μm. (a) was obtained at ambient pressure and (b) was obtained at 5×10^{-6} torr. The images indicate a primary periodicity of 3200Å.

deposition temperature T and the melting temperature T_m) of the metal. For values of τ less than 0.2, the film is believed to be composed of columnar crystallites running throughout the depth of the film. The image of Figure 5 was taken at $\tau = 0.14$; the columnar structure of the film is evident from the scans. The image indicates a lateral size of the columns of about 120 Å, with an average column height of about 70 Å. At this low value of τ, the roughness of the film is found to increase with the thickness of the deposited material, at least up to a thickness of about 200 Å, in accord with the model.

The production of Si integrated circuits often requires the etching into Si wafers of depressions having μm-scale anisotropic features. Illustratively, use is made of preferential etching in a high-pressure plasma discharge containing a fluorocarbon gas to obtain well-defined fine-line profiles. **Figure 6** depicts a pair of STM images of a p-type Si(100) sample which was etched to expose (111) surfaces in a triangular-appearing profile. The sample was air-transported from the plasma chamber to the STM. The images were taken at ambient pressure and 5×10^{-6} torr, respectively. The similarity of the images indicates that the oxide and contamination layers which must have been present under exposure to air at ambient pressure did not play an important role in the imaging process.

The main periodicity of the profile (3200 Å) is apparent from the data, but finer structure with a rather regular

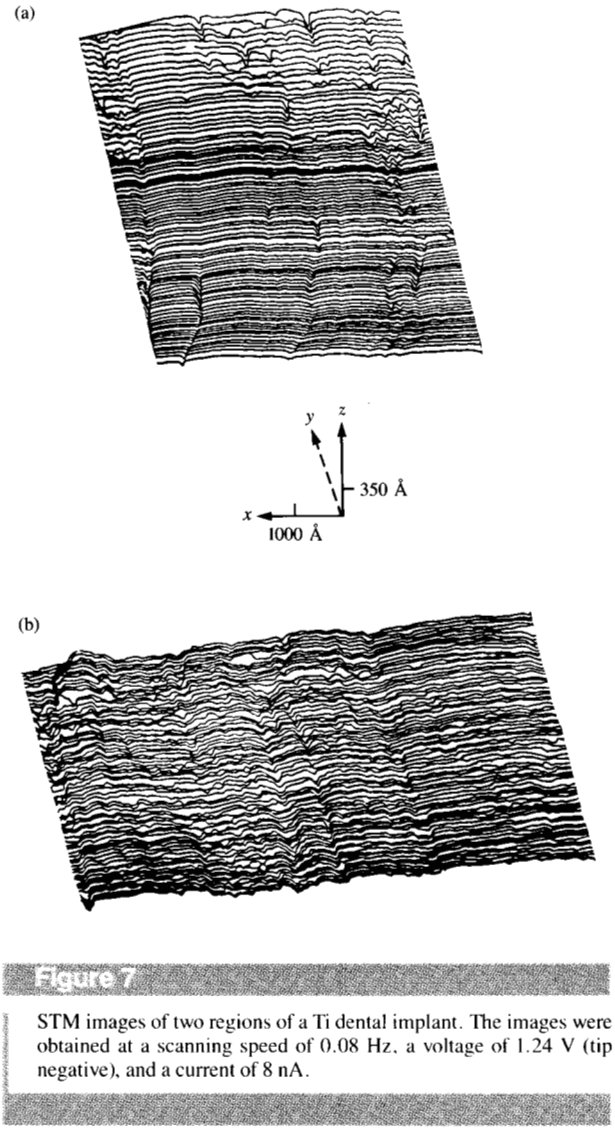

Figure 7

STM images of two regions of a Ti dental implant. The images were obtained at a scanning speed of 0.08 Hz, a voltage of 1.24 V (tip negative), and a current of 8 nA.

spacing of 600–800 Å is clearly detected. The corrugation observed appears only in the direction shown in the figure.

The final example to be discussed is related to medical technology. A factor which has been claimed [15] to be of the highest importance in determining the success of clinical implants is the structure and composition of the outermost surface layer of the implants (criteria for success being the duration without significant wear or corrosion by body fluids). It has been shown [16] that pure Ti implants, when inserted into human bone (mandibular, maxillary, tibial, temporal sites), produce good, direct contact with the bone tissue. The clinical success rate depends on surface preparation and is about 90% for implants whose surface is covered with an oxide layer 50 Å thick.

Recently, we have used the STM to examine the surface topography of surgical dental implants of polycrystalline Ti which have been subjected to different surface treatments [17]. Appreciably different amounts of roughness were found depending on the type of treatments used after machining into clinical shapes (threaded screws). In addition to the machining, the preparation of the clinical samples included ultrasonic cleaning in different solvents and autoclaving at 130–140°C for about 10 minutes.

Figure 7 shows STM images of two different regions of the surface of a Ti clinical sample. The images indicate that the surface is inhomogeneous, with topographic variations on different scales. The region depicted in part (a) appears to be relatively smooth compared to that depicted in part (b), which contains steps and grooves up to about 0.1 μm in depth.

Although no clear correlation has yet been established between surface microstructure and biocompatibility, our results suggest that the smoother the sample, the better the clinical results. It is, however, clear that careful control of all relevant parameters (material design, surgical technique, status of the bone, loading conditions) will be needed before clearcut conclusions can be drawn from these studies.

Concluding remarks

The topological images obtained using the STM in air at ambient pressure indicate that it may have broad applicability to surface analysis. Those obtained from structures derived from bacteriophage ϕ29 demonstrate its potential applicability to biology; others demonstrate its potential applicability to a number of areas of interest in technology, including its possible use as a new standard instrument for surface roughness measurements. The lateral resolution obtained in air at ambient pressure is estimated to be of the order of 20 Å, although that should not be considered as a limit [18].

Acknowledgments

The active interest and constant stimulation by N. García has been of fundamental importance in the development of this work. We thank G. Binnig, H. Rohrer, and Ch. Gerber of the IBM Zurich Research Laboratory for their invaluable help during the early stages of this work and continuous sharing with us of their knowledge of the STM. Image processing was carried out by E. Stoll and A. Brunner of that laboratory. The calibration of the piezoelectric drives which were used was carried out by S. Vieira. The etched Si wafers which were used were kindly provided to us by U. Mockens and D. Heitman. The work on dental prostheses is part of a joint project with C. Aparicio, J. Olivé, and J. Lausmaa. We thank L. Vázquez, J. Presa, and J. Alamán for their help with various aspects of the experiments. Finally, financial support from the IBM Corporation and the Ramon Areces Foundation is gratefully acknowledged.

References and notes

1. G. Binnig, H. Rohrer, Ch. Gerber, and E. Weibel, *Appl. Phys. Lett.* **40,** 178 (1982).
2. See for example other papers in this and the September issue of *IBM J. Res. Develop.*
3. G. Binnig, H. Rohrer, Ch. Gerber, and E. Weibel, *Phys. Rev. Lett.* **49,** 57 (1982).
4. J. Moreland, S. Alexander, M. Cox, R. Sonnenfeld, and P. K. Hansma, *Appl. Phys. Lett.* **43,** 387 (1983).
5. G. Binnig and H. Rohrer, *Surf. Sci.* **126,** 236 (1983).
6. A. M. Baró, R. Miranda, J. Alamán, N. García, G. Binnig, H. Rohrer, Ch. Gerber, and J. L. Carrascosa, *Nature* **315,** 253 (1985).
7. D. L. Anderson, D. D. Hickman, and B. E. Reilly, *J. Bacteriol.* **91,** 2089 (1966).
8. J. L. Carrascosa, E. Viñuela, N. García, and A. Santisteban, *J. Molec. Biol.* **154,** 311 (1982).
9. J. L. Carrascosa, J. M. Carazo, C. Ibáñez, and A. Santisteban, *Virology* **141,** 190 (1985).
10. *Handbook of Industrial Metrology*, J. W. Grove, Ed., Prentice-Hall, Inc., Englewood Cliffs, NJ, 1967.
11. N. García, A. M. Baró, R. Miranda, H. Rohrer, Ch. Gerber, R. Garcia, and J. L. Peña, *Metrologia* **21,** 566 (1985).
12. See for example C. J. Kircher and S. K. Lahiri, *IBM J. Res. Develop.* **24,** 235 (1980).
13. R. Miranda, N. García, A. M. Baró, R. Garcia, J. L. Peña, and H. Rohrer, *Appl. Phys. Lett.* **47,** 367 (1985).
14. J. V. Sanders, in *Chemisorption and Reactions on Metallic Films*, Academic Press, London, 1971.
15. B. Kasemo, *J. Prosth. Dent.* **49,** 832 (1983).
16. *Tissue Integrated Prostheses: Osseointegration in Clinical Dentistry*, P. I. Branemark, G. A. Zarb, and T. Albrektsson, Eds., Quintessence Publishing Co., Inc., Chicago, 1985.
17. C. Aparicio, J. Olivé, J. Lausmaa, A. M. Baró, N. García, R. Miranda, and L. Vázquez, *Biomaterials*, accepted for publication.
18. Note added in proof: Since this paper was written, a substantial improvement has been reported in the resolution which can be achieved in air. In particular, Sang-Il Park and C. F. Quate [*Appl. Phys. Lett.* **48,** 112 (1986)] have obtained STM images of highly oriented graphite in air at ambient pressure at a lateral resolution of less than 2 Å.

Received July 5, 1985; accepted for publication October 21, 1985

Artur M. Baró *Autonomous University of Madrid, Department of Fundamental Physics, C-III, Cantoblanco, 28049 Madrid, Spain.*
Dr. Baró has been with the Universidad Autónoma de Madrid (UAM) since 1970. Prior to that he carried out studies on secondary electron emission at the Université de Toulouse, France. He received his Ph.D. in physics from the UAM in 1974. From 1978 to 1980 he held a Humboldt Fellowship, carrying out postdoctoral studies in the IGV der Kernforschungsanlage, Jülich, Federal Republic of Germany. His research interests include surface science, particularly vibrational spectroscopy. In 1983 he was a visiting scientist at the IBM Research Laboratory in Rüschlikon, Switzerland. At present he is supervising a project on biological and technological applications of scanning tunneling microscopy.

Rodolfo Miranda *Autonomous University of Madrid, Department of Fundamental Physics, C-III, Cantoblanco, 28049 Madrid, Spain.*
Dr. Miranda has been with the Universidad Autónoma de Madrid (UAM) since 1975. He received his Ph.D. in physics from the UAM in 1980. From 1982 to 1984 he held a Humboldt Fellowship at the Institut für Physikalische Chemie der Universität München. He has also been involved with several projects in the Synchrotron Radiation Laboratory in Berlin and Paris. His current interests include surface science, particularly photoemission spectroscopy.

Jose Lopez Carrascosa *Autonomous University of Madrid, C.S.I.C., Center for Molecular Biology, Cantoblanco, 28049 Madrid, Spain.*
Dr. Carrascosa received his Ph.D. from the Universidad Complutense de Madrid in 1976. From 1976 to 1979 he carried out postdoctoral studies in the Biozentrum der Basel Universität with Professor Kellenberger. In 1979 he joined the Centro de Biología Molecular, where he is at present supervising the electron microscopy group. His current interests include viral ultrastructure and morphogenesis, and the use of scanning tunneling microscopy for biological studies.